Journal of Alloys and Compounds, 211/212 (1994) 628–631
JALCOM 097

Varying ultrasonic attenuation in welds with nickel filler metal

V.A.M. Luprano and G. Montagna
CNRSM, Centro Nazionale per la Ricerca e la Sviluppo dei Materiali, SS 7 per Mesagne, I-72100 Brindisi (Italy)

Abstract

Electron beam welds with two different contents of nickel filler metal were observed by scanning laser acoustic microscopy (SLAM). Acoustic images at 10 and 30 MHz were obtained. The different ultrasonic attenuation along the welds was ascribed to the different metallographic structure and to scattering by grains. Optical images have also shown a different surface structure and morphology in the welds. Therefore microhardness measurements and ultrasonic attenuation seem to follow an equivalent profile along the same weld lines.

In conclusion, SLAM proves to be an effective non-destructive tool in the investigation of structural changes and mechanical properties.

1. Introduction

This paper is concerned with detecting changes in the anisotropy factor occurring during rapid cooling of Fe460 welds with 4% and 25% contents of nickel filler metal.

1.1. Background

Usually, a filler metal in welding alloys provides several advantages, *e.g.* uniform mechanical properties throughout the weld joint and the base metal after post-weld heat treatment and increases in tensile strength, hardness and fatigue strength.

To improve the mechanical properties of iron–carbon alloys, experience shows that it is useful to add nickel filler metal in an amount not greater than 12% [1]. This happens because different massive transformations (*e.g.* martensite, bainite, pearlite and so on) occur during the weld solidification process depending on the nickel content and the cooling rate [2].

In fact, crystalline transformations of iron occur in the majority of steels and give, during cooling, various superimposed structures. Usually it is possible to distinguish [3] (i) the primary or solidification structure (δ dendrites) and (ii) secondary grains formed by complete transformation to γ-austenite. When a fast cooling rate is used, the martensite structure can grow in the secondary grains.

The solidification process after electron beam welding appears as columnar grain (dendrite) growth in the direction of the thermal gradient, with the grains growing epitaxially from the base metal towards the heating source. If the diffusion during cooling is low, a significant solute enrichment occurs in the intercellular liquid region. Thus, depending on the nickel content, a new phase of higher composition can nucleate in the intercellular regions.

1.2. Present investigation

A scanning laser acoustic microscope (SLAM) system was used to detect changes in the metallographic structure due to the different processes of grain growth depending on the nickel content in the welds. The ultrasonic attenuation depends on the anisotropy factor of the grains [4] according to the following formulae.

For Rayleigh scattering with $\lambda > 2\pi D$,

$$\alpha = A\mu^2 D f^4 + F(f) \quad (1)$$

where A is a constant involving the velocity and density, μ is the anisotropy factor depending on the crystallographic structure, D is a suitable average grain volume, f is the ultrasonic frequency and $F(f)$ is function of frequency arising from the thermoelastic loss, etc. [5].

For stochastic scattering with $\lambda < 2\pi D$,

$$\alpha = A\mu^2 D f^2 + F(f) \quad (2)$$

Since the martensite structure has more isotropic elastic properties than the dendrite structure [6] and a different grain size, the different scattering from the grains can be attributed to the presence of either martensite or dendrites.

2. Experimental details

The acoustical analysis was performed by scanning laser acoustic microscopy (SLAM) using a Sonomicro-

SSDI 0925-8388(93)00097-I

scope System 2140 manufactured by Sonoscan Inc., IL, USA. The SLAM uses the propagation of continuous plane ultrasonic waves at frequencies of 10, 30 and 100 MHz to detect changes in the structure [7], defects and different metallographic phases inside the sample. A scanning laser beam is used as an ultrasound detector by means of sensing the displacements (rippling) of the surface created by transmission of the ultrasonic waves [8].

Ultrasonic attenuation measurements were also performed by the pulse echo method.

The electron-beam-cast welds were obtained using Fe460 as base metal and nickel at two different concentrations as filler metal. Scanning electron microscopy (SEM) analysis has shown that the concentration of Ni in sample 1 was 4% throughout the weld. In contrast, in sample 2 it was 24% at the weld top and 21% at the weld bottom. Both samples were polished using 6 and 3 μm diamond paste on hard nylon cloths. Sample 1 was etched in Nital for 6 s, sample 2 for 10 s.

Microhardness measurements were performed by applying a load of 0.300 kgf for 15 s.

3. Results and discussion

Samples 1 and 2 were observed by SLAM at frequencies of 10 and 30 MHz (Figs. 1–4). The brighter zones correspond to a lower attenuation. A higher resolution is obtained at higher working frequencies because the wavelength is lower.

3.1. Sample 1

At 30 MHz the weld bead (Fig. 2, central part) shows a low ultrasonic attenuation that can be explained via the structure revealed by optical micrography. The primary (dendrites; columnar grains corresponding to the rows in Fig. 5) and secondary (martensite structure) phases were detected. As seen in the phase diagram

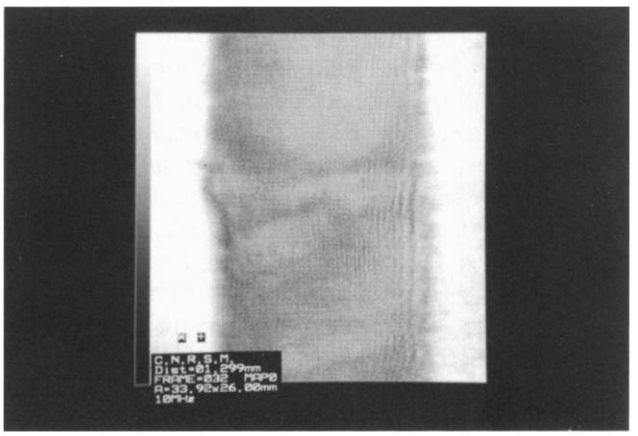

Fig. 2. Sample 1: acoustic micrograph taken at 30 MHz.

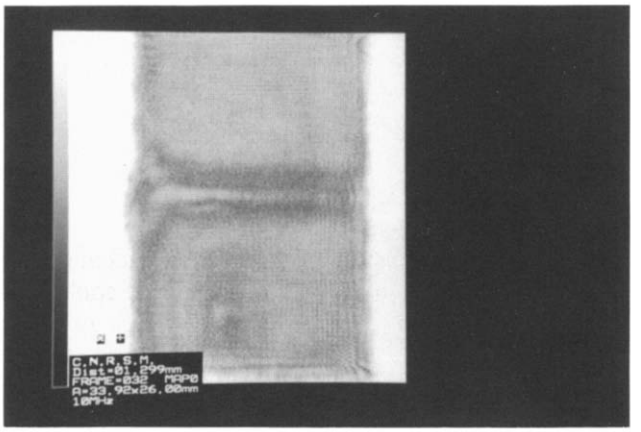

Fig. 3. Sample 2: acoustic micrograph taken at 10 MHz.

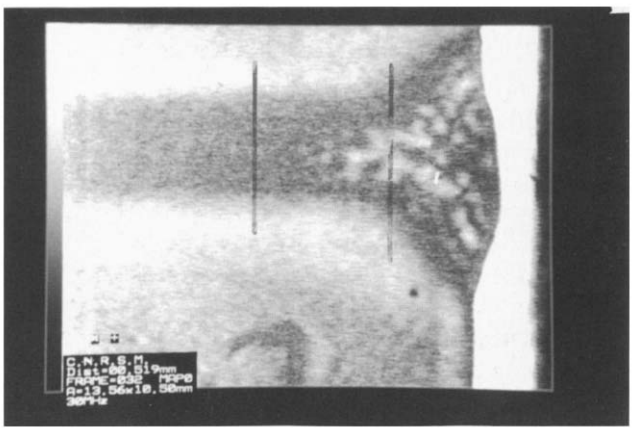

Fig. 4. Sample 2: acoustic micrograph taken at 30 MHz.

(Fig. 6), with 4% Ni content a transformation in the δ phase occurs. In this phase the growth of the secondary grains in which the martensite structure grew [3], which is also confirmed by the values from the microhardness measurements (Fig. 7). One can infer that this structure produces a low attenuation because of its low anisotropy factor.

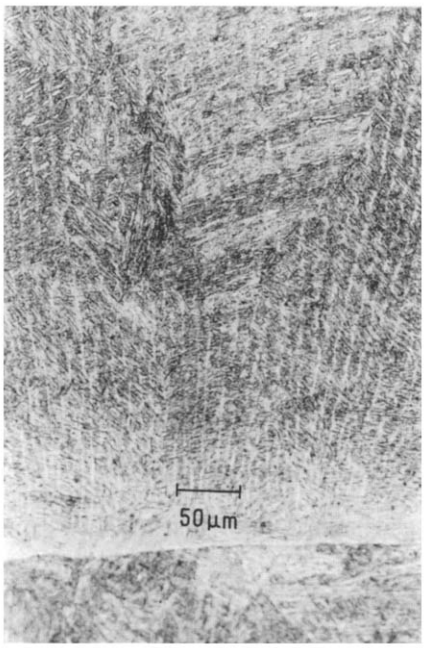

Fig. 5. Sample 1: optical micrograph.

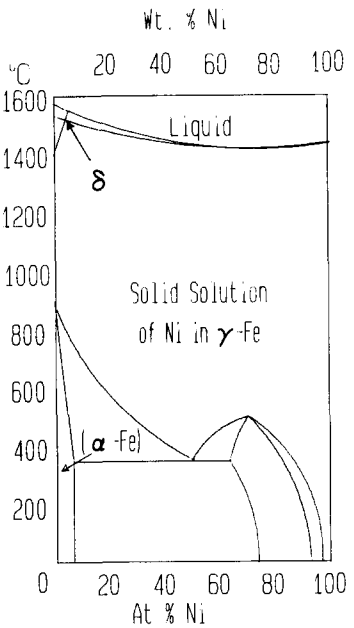

Fig. 6. Fe–Ni phase diagram.

3.2. Sample 2

In Fig. 4 one can observe that the weld bead top presents a lower attenuation than the bottom. By means of optical observations, the microsegregations developed during the non-equilibrium solidification of the weld were identified. Microsegregations are characterized by a compositional difference between the cores and peripheries of cellular dendrites [9]. Since at 25% Ni content there is no transition in the δ phase but there is an enrichment of nickel content in the dendrite grain boundaries, the martensite structure grows only at the

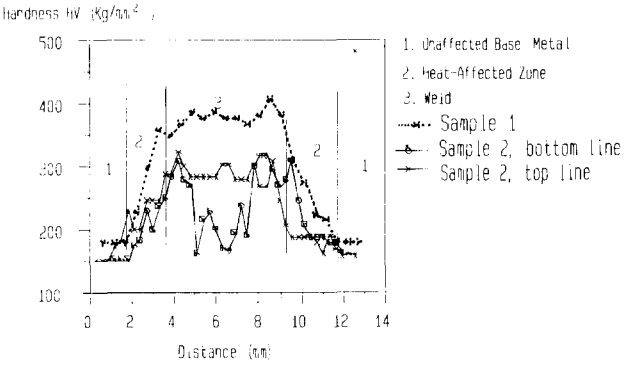

Fig. 7. Microhardness measurements along weld beads.

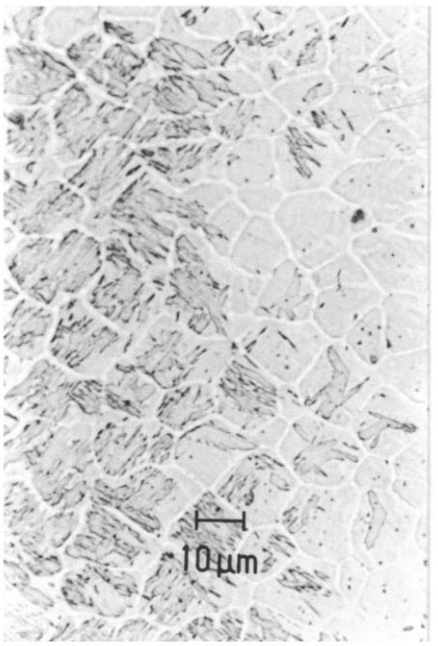

Fig. 8. Sample 2: optical micrograph.

boundaries and inside the dendrites as seen in Fig. 8. The presence or absence of martensite was also confirmed by microhardness measurement along two weld bead lines (top and bottom) (Fig. 7). Patches of the massive phase extend on both sides of the prior parent grain boundary, indicating that the growth of the massive phase is unaffected by orientation relationships between the parent and the product phase [10]. The martensite grew in the region where the thermal gradient was higher. As seen in the optical micrograph, over all the bead top the martensite grew inside the dendrites, because in this zone the temperature gradient was higher than at the bottom. Also at 10 MHz (Fig. 3) one can see the profile of the martensite structure (central bright zone inside the weld) and the difference from the sample 1 weld (Fig. 1).

Thus it is possible to deduce that the low anisotropy factor in the martensite produces a lower ultrasonic attenuation. From the point of view of ultrasonic scat-

tering theory [6, 11], the randomization should give rise to a decrease in the elastic anisotropy of the prior grain volume and consequently to a decrease in the scattering. The Rayleigh-scattering theoretical calculation confirms the values from the ultrasonic attenuation measurements. We considered Rayleigh scattering (eqn. (1)) for sample 2 because the wavelength is higher than the grain size. In contrast, stochastic scattering (eqn. (2)) was considered for sample 1.

In both acoustic micrographs at 30 MHz one can observe the heat-affected zone (brighter zone outside the welds).

4. Conclusions

Differences in elastic properties and density are very important for determining the properties of solids. These differences can be associated both with crystal defects extending from larger sources, *e.g.* grain boundaries, precipitates and inhomogeneities in composition, and with changes in crystallographic structures. The SLAM can be considered as an important system not only to detect internal defects with a very high resolution greater than (25 μm) but also to point out non-destructively different metallographic structures. In fact, the martensite structure was distinguished from the dendrite one by the different ultrasonic attenuation owing to the correspondence between mechanical properties and ultrasonic transmission properties.

Acknowledgments

The authors would like to thank Dr. F. De Riccardis of CNRSM Electron Microscopy Laboratory for the SEM analysis and the CNRSM Mechanical Characterization Laboratory for the microhardness measurements. The authors would also like to thank Dr. J. Marrow of Oxford University for interesting discussions.

References

1 D. Lucchesi, *Tecnologia Meccanica,* Vol. 3, Sansoni Editore, 1987, p. 251.
2 J.H. Devletion and W.E. Wood, Principles of joining metallurgy, in *Metals Handbood,* Vol. 6, American Society for Metals, Metals Park, OH, 9th end., 1983, p. 26.
3 De Ferri, *Metallographia,* Vol. 3, Berger Levrault, Paris, p. 40.
4 W.P. Mason and H.J. McSkimin, *J. Acoust. Soc. Am., 19* (1947) 464.
5 E.P. Papadakis, Ultrasonic attenuation caused by scattering in polycrystalline media, in W.P. Mason (ed.), *Physical Acoustics,* Vol. 4, Pt. B, Academic, New York, 1968, p. 269.
6 E. Papadakis and E.L. Reed, Ultrasonic detection of changes in the elastic properties of a 70–30 iron–nickel alloy upon heat treatment, *J. Appl. Phys., 32*(4) (1961) 682.
7 L.W. Kessler, Acoustic microscopy – 1979, *Proc. IEEE, 67*(4) (1979) 526–536.
8 L.W. Kessler, Imaging with dynamic-ripple diffraction, in *Acoustical Images,* Vol. 16, Plenum, New York, 1976, Chap. 10, pp. 229–239.
9 J.S. Langer, Recent developments in the theory of dendritic solidification, in *Crystall Properties and Preparation,* Aedermanns Dorf, Switzerland, Vols. 22–25, Pt. 1, Trans Tech, 1990, p. 2.
10 T.B. Massalki, Massive transformation structures, in *Metals Handbook,* Vol. 9, American Society for Metals, Metals Park, OH, 9th edn., 1985, p. 655.
11 E. Papadakis, Ultrasonic attenuation and velocity in three transformation products in steel, *J. Appl. Phys., 35*(5) (1964) 1474.